

Identification of a host protein essential for assembly of immature HIV-1 capsids

Concepcion Zimmerman*, Kevin C. Klein†, Patti K. Kiser†, Aalok R. Singh*, Bonnie L. Firestein‡, Shannyn C. Riba† & Jaisri R. Lingappa†§

* Department of Physiology, University of California at San Francisco, San Francisco, California 94143, USA

† Department of Pathobiology, University of Washington School of Public Health; and § Department of Medicine, Division of Allergy and Infectious Disease, University of Washington School of Medicine Seattle, Washington 98195, USA

‡ Department of Cell Biology and Neuroscience, Rutgers University, Piscataway, New Jersey 08854, USA

To form an immature HIV-1 capsid, 1,500 HIV-1 Gag (p55) polypeptides must assemble properly along the host cell plasma membrane. Insect cells and many higher eukaryotic cell types support efficient capsid assembly¹, but yeast² and murine cells^{3,4} do not, indicating that host machinery is required for immature HIV-1 capsid formation. Additionally, in a cell-free system that reconstitutes HIV-1 capsid formation, post-translational assembly events require ATP and a subcellular fraction⁵, suggesting a requirement for a cellular ATP-binding protein. Here we identify such a protein (HP68), described previously as an RNase L inhibitor⁶, and demonstrate that it associates post-translationally with HIV-1 Gag in a cell-free system and human T cells infected with HIV-1. Using a dominant negative mutant of HP68 in mammalian cells and depletion–reconstitution experiments in the cell-free system, we demonstrate that HP68 is essential for post-translational events in immature HIV-1 capsid assembly. Furthermore, in cells the HP68–Gag complex is associated with HIV-1 Vif, which is involved in virion morphogenesis and infectivity. These findings support a critical role for HP68 in post-translational events of HIV-1 assembly and reveal a previously unappreciated dimension of host–viral interaction.

Previously, we established a cell-free system for translation and assembly of HIV-1 Gag polypeptides into immature HIV-1 capsids—the protein shells that protect the viral genome^{5,7}. In this system, ATP is required post-translationally for capsid assembly⁵. Because HIV-1 Gag is not thought to bind ATP, a cellular protein is probably involved. To determine whether a cellular nucleotide-binding protein is associated with assembling HIV-1 Gag chains, we examined whether antibodies directed against various ATP-binding molecular chaperones co-immunoprecipitate radiolabelled Gag in this system. Only one antibody (23c) co-immunoprecipitated Gag under native conditions, but not after denaturation (which disrupts protein–protein interactions). This antibody recognizes an epitope (containing LDD-COOH) present in several eukaryotic proteins, including the molecular chaperone TCP-1 (refs 8, 9). 23c failed to co-immunoprecipitate other substrates translated in the cell-free system, and recognized a 68K (relative molecular mass (M_r) of 68,000) wheatgerm protein by immunoblotting and immunoprecipitation (see Supplementary Information Fig. 1).

Capsids formed during a cell-free assembly reaction closely correspond to authentic, immature HIV-1 capsids by biochemical and morphological criteria⁵. In the cell-free system, which uses wheatgerm extract as a source of cellular factors, 750S completed capsids are produced by means of a stepwise pathway of post-translational, Gag-containing complexes (10S, 80S, 150S and 500S). These complexes, which behave as true assembly intermediates⁵, are absent during the synthesis phase of the reaction; they accumulate after translation, and then diminish^{5,7}. Co-immunoprecipitations,

using 23c, performed at different times during a pulse-chase assembly reaction suggested that Gag associates with HP68 only transiently, when assembly intermediates are at high levels, releasing HP68 once assembly is completed (see Supplementary Information Fig. 2). Co-immunoprecipitation of fractions produced by velocity sedimentation of assembly reaction products revealed that Gag was associated with HP68 in 80S and 500S (but not 10S or 750S) peak fractions (see Supplementary Information Fig. 2). Hepatitis B virus (HBV) core, which forms assembly intermediates and capsids that are fully assembled in the cell-free system¹⁰, was not co-immunoprecipitated by 23c (data not shown). Thus, HP68 associates selectively with partially assembled, post-translational HIV-1 capsid assembly intermediates, but not with unassembled Gag, fully assembled HIV-1 capsids, or HBV capsid assembly intermediates. These data suggest a specific role for HP68 in post-translational events of HIV-1 capsid assembly.

Wheatgerm HP68 (WGHP68) was isolated from wheatgerm extracts by immunoaffinity purification using 23c antibody, and microsequenced. Degenerate oligonucleotides were used to amplify a 2-kilobase (kb) complementary DNA from wheatgerm cDNA. The deduced amino-acid sequence (see Supplementary Information Fig. 3) was 71% identical to cDNA coding for the 68K human RNase L inhibitor⁶ (termed here HuHP68). Both WGHP68 and HuHP68 contain two ATP/GTP-binding motifs¹¹ as well as the

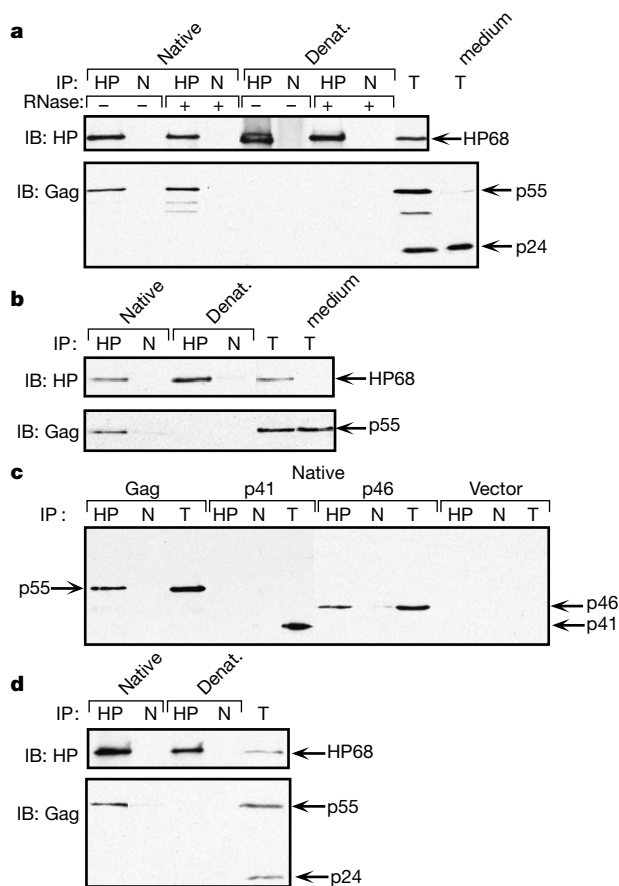


Figure 1 Anti-HuHP68 co-immunoprecipitates HIV-1 Gag in mammalian cells. **a–d**, Native or denaturing (Denat.) immunoprecipitations (IP) on cell lysates using anti-HuHP68b (HP) or non-immune serum (N), followed by immunoblotting with antibody to HuHP68 (immunoblot (IB): HP) or Gag (IB: Gag). HIV-1 p24 and p55, 5% input cell lysate (T), and 10 μ l medium (T medium) are indicated. **a**, 293T cells transfected with pBRU Δ env, with or without RNase A treatment. **b**, Cos-1 cells expressing Gag. **c**, Cos-1 cells expressing Gag, an assembly-incompetent Gag mutant (p41), an assembly-competent Gag mutant (p46), or control vector (native immunoprecipitation only). **d**, ACH-2 cells chronically infected with HIV-1.

LDD-_{COOH} epitope. HuHP68 binds and inhibits RNase L⁶—an interferon-dependent nuclease associated with polysomes^{12,13} whose activation results in viral RNA degradation¹⁴. Antisense knockouts of RNase L inhibitor in cells that are infected with HIV-1 block virion production by reducing levels of HIV-1 RNA and HIV-1-specific proteins¹⁵. However, this fails to explain why WGHP68 binds to post-translational intermediates during cell-free HIV-1 capsid assembly. Thus, we investigated whether HuHP68 binds to and acts on fully synthesized Gag chains after translation in cells, in addition to binding and inhibiting RNase L as described previously⁶.

We generated polyclonal antisera that specifically recognize the carboxy terminus of WGHP68 or HuHP68 (see Supplementary Information Fig. 3). 293T cells were transfected with a plasmid (pBRUΔenv) encoding the entire HIV-1 genome except a region of the envelope gene¹⁶. Affinity-purified antisera to HuHP68 that was coupled to protein A beads (anti-HuHP68b) co-immunoprecipitated HIV-1 Gag from cell lysates under native conditions, but not after denaturation (Fig. 1a). Neither degradation of messenger RNA with RNase A (Fig. 1a) nor disassembly of ribosomes with EDTA (see below) affected HP68–Gag binding, indicating that this association does not require polysome integrity. Furthermore, HP68 did not associate with incomplete, nascent Gag chains (data not shown). Thus, HP68 appears to associate with Gag after translation. In addition, HP68–Gag binding occurred in the absence of other viral proteins, as seen in the cell-free system (see Supplementary Information Fig. 1) and in cells that express p55 Gag and produce immature HIV-1 virions¹⁷ (Fig. 1b). Furthermore, HP68 bound an assembly-competent Gag mutant (p46) that lacks the p6 domain, but did not bind the assembly-incompetent p41 Gag mutant that lacks both the nucleocapsid (NC) and p6 domains^{5,18–21} (Fig. 1c). Finally, HP68 associated with Gag in human T cells (ACH-2) that were producing infectious HIV-1 (Fig. 1d). Thus, HP68–Gag binding was seen in all of the HIV-1 capsid-producing systems that we examined.

We confirmed HP68–Gag co-association using immunofluorescence microscopy. In Cos-1 cells, Gag was expressed in a predominantly clustered pattern (Fig. 2b, e), probably representing Gag localization to sites of virus formation at the plasma membrane. HP68 labelling revealed a diffuse pattern in all cells not expressing Gag (see Fig. 2a, two cells on the left), and a coarsely clustered pattern in Gag-expressing cells (Fig. 2d). Merged images revealed co-localization of HP68 with Gag in these clusters (Fig. 2c, f; yellow). This recruitment of HP68 by Gag was seen in 100% of

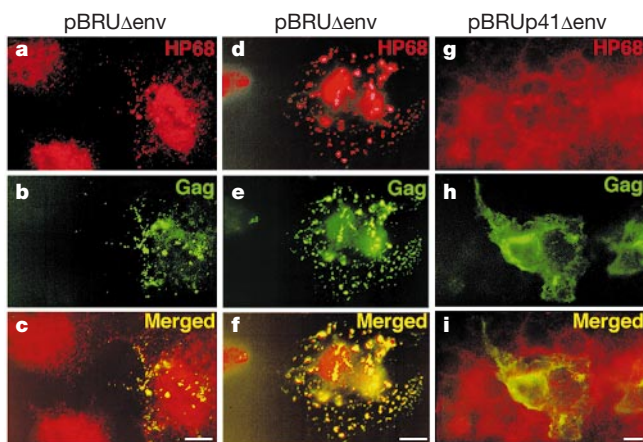


Figure 2 Co-localization of HP68 with HIV-1 Gag in mammalian cells. Cos-1 cells were transfected with pBRUΔenv or pBRUp41Δenv (truncated proximal to the nucleocapsid domain in Gag), and double-label indirect immunofluorescence was performed. Cells were labelled for HP68 (a, d, g; red), or Gag (b, e, h; green). Images were merged to show overlap of HP68 and Gag labelling (c, f, i; yellow). Scale bars, 50 μm.

cells displaying HIV-1 Gag clusters, but not in any cells expressing the p41 assembly-incompetent Gag mutant (Fig. 2g–i).

To examine the function of HP68, we co-transfected truncated WGHP68 that encoded a stop codon before the second nucleotide-binding domain (WGHP68-Tr1) along with Gag expression plasmids into Cos-1 cells. We chose WGHP68 because it can be distinguished from endogenous HP68 using specific antisera. Furthermore, at low levels of expression it is less effective as an RNase L inhibitor than HuHP68 (data not shown), allowing post-transcriptional and post-translational effects of HP68 to be dissociated. Increasing expression of WGHP68-Tr1 resulted in a 4.7-fold dose-dependent decrease in the amount of HIV-1 Gag in the medium (Fig. 3a). Gag and actin levels in cell lysates remained unchanged (Fig. 3b), indicating that the effect of WGHP68-Tr1 is not mediated by changes in Gag synthesis or degradation, and that WGHP68-Tr1 is not toxic to cells. Similar results were obtained when pBRUΔenv and WGHP68-Tr1 were co-expressed in human cells (Fig. 3c, d). The dose-dependent decrease in p24 release was reversed on co-expression of wild-type WGHP68 with these plasmids (data not shown). The reduction in virion formation resulting from WGHP68-Tr1 expression while Gag levels are unchanged suggests that HP68 promotes virion formation by a post-translational mechanism. Co-immunoprecipitation of Gag with epitope-tagged WGHP68-Tr1 confirmed that WGHP68-Tr1 competes with wild-type HP68 for binding to

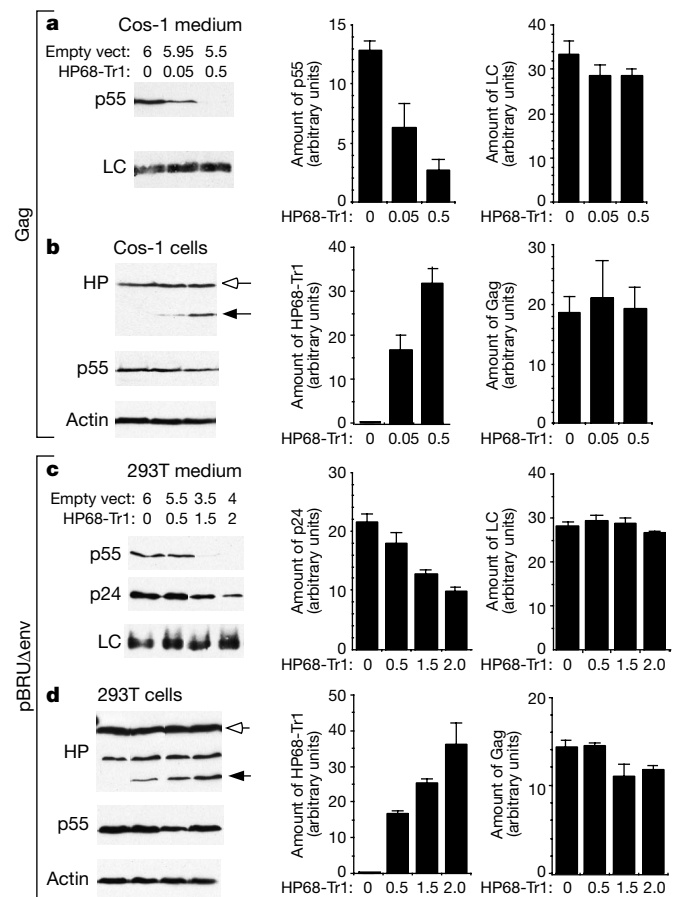


Figure 3 Truncated HP68 blocks virion production. a–d, Cos-1 (a, b) or 293T (c, d) cells co-transfected with varying amounts (μg) of plasmid expressing WGHP68-Tr1 and empty vector, as indicated, plus plasmids for expression of HIV-1 Gag (a, b) or pBRUΔenv (c, d). Medium (a, c) was immunoblotted with Gag antibody (p55, p24), and reprobed with antibody to light-chain tracer (LC). Cell lysates (b, d) were immunoblotted using WGHP68 antiserum (HP) or Gag antibody (p55, p24), and reprobed using actin antibody (actin). White arrows indicate endogenous HP68; black arrows indicate WGHP68-Tr1 (a cross-reacting band can also be seen). Graphs represent blots from three experiments quantified using sample dilution standard curves.

HIV-1 Gag (data not shown).

The dominant negative effect of WGHP68-Tr1 on virion formation (Fig. 3) indicates an essential role for HP68 in post-translational events in virion formation, but does not distinguish between HP68 acting on capsid assembly versus virus budding. For this, we used biochemical manipulation of the cell-free system. As wheatgerm extract does not contain functional RNase L⁶, HP68 in this system does not act as an inhibitor of RNase L. Immunodepletion of wheatgerm extract reduced levels of WGHP68 by 70% (data not shown). Immunodepletion had no effect on Gag translation (Fig. 4a), but reduced the amount of 750S completed capsids by 60% (Fig. 4b). Furthermore, the depleted reaction was arrested at the 500S assembly intermediate, with accumulation of 10S and 80S intermediates, but no formation of 750S completed capsids (Fig. 4b, c). The small amount of Gag seen in the 750S position using

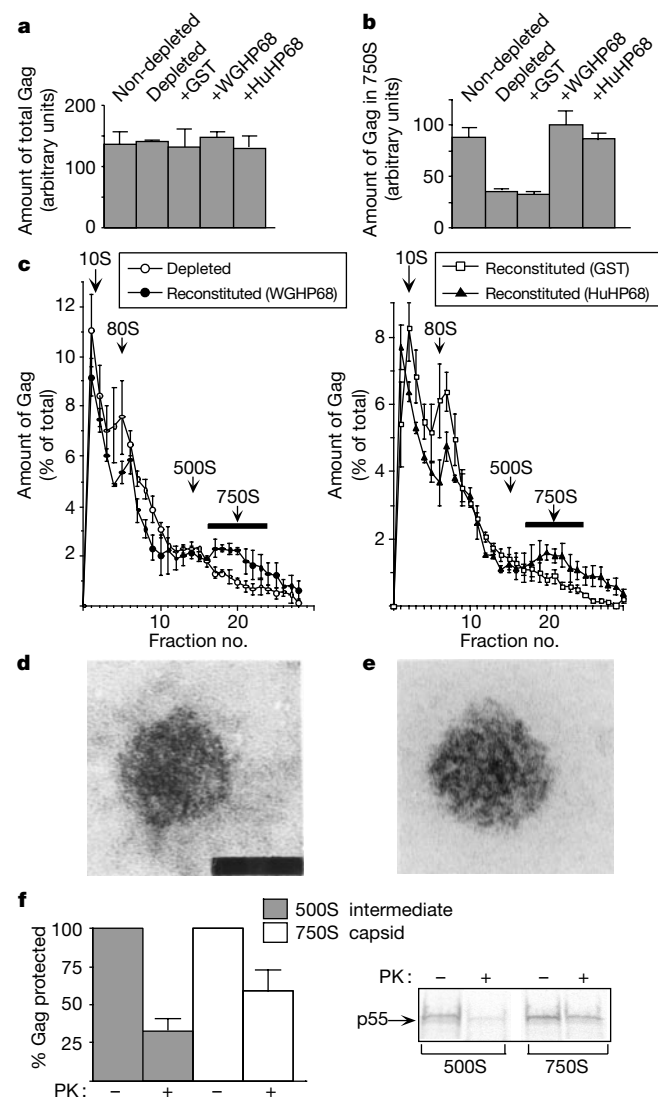


Figure 4 HP68 depletion–reconstitution. **a, b**, Graphs showing total Gag synthesized (**a**) or amount of Gag in 750S completed capsids (**b**) from cell-free reactions programmed with indicated wheatgerm extracts. Non-depleted; depleted, immunodepleted of HP68; +GST, immunodepleted and reconstituted with GST alone; +WGHP68, depleted and reconstituted with WGHP68–GST; +HuHP68, depleted and reconstituted with HuHP68–GST. **c**, Amount of Gag in fractions from cell-free reactions in **a** that were subjected to velocity sedimentation. **d, e**, Transmission electron microscopy of capsids from immunodepleted cell-free reactions reconstituted with WGHP68–GST (**d**) or immature capsids from transfected mammalian cells (**e**). Scale bar, 100 nm. **f**, Proteinase K (PK) digestion of 500S and 750S fractions shown as percentage of Gag protected relative to normalized controls.

depleted extract was due to a trail from the 500S complex that enters the 750S region (Fig. 4b, c). Immunodepletion of HP68 had no effect on HBV capsid assembly (data not shown). Addition of purified recombinant WGHP68–glutathione S-transferase (GST) or HuHP68–GST to reactions programmed with immunodepleted extract produced a threefold increase in the amount of 750S capsid, restoring 750S capsids to levels seen in non-depleted extracts (Fig. 4c and data not shown). This reconstitution had no effect on Gag synthesis, indicating a post-translational action (Fig. 4a). Electron microscopy confirmed the absence of capsids in immunodepleted reactions (data not shown) and their presence in reconstituted reactions (Fig. 4d, e). Proteinase K digestion (Fig. 4f) revealed that the 500S capsid assembly intermediate (the end product of immunodepleted reactions) was protease-sensitive, whereas the 750S capsid produced by standard or reconstituted reactions was relatively resistant to protease treatment. This suggests that HP68-mediated conversion of Gag into completed 750S immature capsids is associated with a change in the conformation of the assembling capsid complex.

If HP68 acts post-translationally on capsid assembly intermediates, then other HIV-1 proteins involved in virion morphogenesis may also be associated with HP68. To test this, lysates of cells expressing pBRUΔenv were immunoprecipitated using anti-HuHP68b (in the presence and absence of EDTA) and immunoblotted for specific viral and cellular proteins. In addition to associating with Gag, HuHP68 associated with HIV-1 Gag-Pol and Vif, but not with Nef, which is probably incorporated into virions by direct association with the plasma membrane^{22–24} (Fig. 5a and data not shown). Furthermore, neither actin nor RNase L were co-immunoprecipitated using anti-HuHP68b (Fig. 5a). Co-immunoprecipitation of Gag-Pol and Vif was inhibited by pre-incubating anti-HuHP68b with HuHP68 peptide, indicating the specificity of these interactions (Fig. 5b).

Our findings support a model in which HIV-1 upregulates a multifunctional cellular protein (HP68), exploiting it to promote critical events at two different stages in the viral life cycle. In

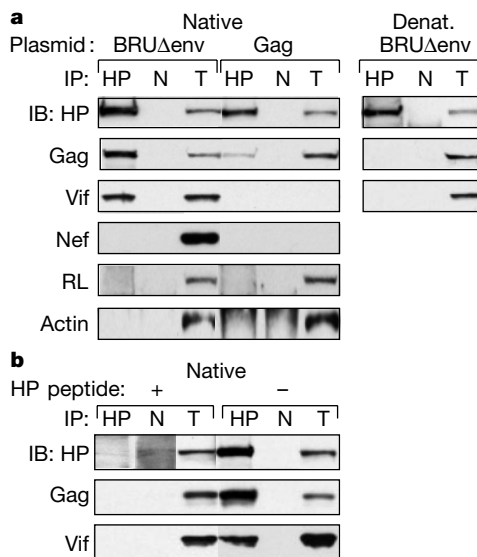


Figure 5 Anti-HuHP68 co-immunoprecipitates HIV-1 Vif but not Nef or RNase L. **a**, Cos-1 cells transfected with pBRUΔenv or Gag plasmids were immunoprecipitated (IP) under native or denaturing (Denat.) conditions using anti-HuHP68b (HP) or non-immune serum (N), and immunoblotted (IB) with antibody to HuHP68 (HP), Gag, Vif, Nef, RNase L (RL), or actin. T, Total (5% of input cell lysate used in immunoprecipitation (IP, 10%)). The top of some actin lanes contain heavy chain cross-reacting to secondary antibody. **b**, Lysates of pBRUΔenv-transfected Cos-1 cells collected in 10 mM EDTA-containing buffer, and co-immunoprecipitated using beads pre-incubated with HuHP68 peptide or diluent control.

addition to acting post-transcriptionally by inhibiting RNase L^{6,15}, HP68 binds Gag after translation and promotes its assembly into immature capsids. This is the first report, to our knowledge, of a cellular factor being essential for post-translational events in HIV-1 capsid assembly. Evidence for this post-translational mechanism comes from genetic (dominant negative), biochemical (depletion-reconstitution) and morphological (electron microscopy) studies presented here. HP68 appears to act during conversion of assembly intermediates into completed immature capsids, promoting a conformational change that may be important for immature capsid integrity or maturation. Thus, HP68 may act as a molecular chaperone during capsid assembly. Data demonstrating that HP68 selectively associates with three viral proteins critical for assembly of a fully infectious virion (Gag, Gag-Pol and Vif) provide further support for a post-translational action. These findings may help with understanding species-specific restriction to virion formation and the function of Vif, which acts during virion assembly by means of an unidentified host factor and is required for formation of virions that are fully infectious *in vivo*^{25–28}. □

Methods

Cell-free assembly reactions

Cell-free translations, pulse chase and velocity sedimentation were performed as described^{5,7,10}.

Purification and sequencing of HP68

For purification, 3 ml of wheatgerm extract supernatant (centrifuged in a Beckman TL100.2 rotor, 15 min, 436,000g), was immunoprecipitated using 50 µg 23c antibody (Stressgen). Immunoprecipitate was transferred to polyvinylidene difluoride membrane; Coomassie staining revealed a single 23c-reactive protein (68K). This protein was microsequenced (ProSeq), found to be amino-terminally blocked, and was treated with cyanogen bromide and *O*-phthalaldehyde, which allowed Edman sequencing of two proline-containing peptides.

cDNA amplification

Degenerate oligonucleotides corresponding to WGHP68 3' sequence were synthesized: 5'-ATGAATTC(CTG)GG(CTG)CG(GA)TA(GA)TT(CTG)GT(CTG)GG(GA)TC-3' and 5'-ATGAATTC(CTG)GG(CT)CT(GA)TA(GA)TT(CTG)GT(CTG)GG(GA)TC-3'. WGHP68 was amplified by PCR, using wheatgerm cDNA (Invitrogen), 3' oligonucleotide corresponding to the WGHP68 C terminus, and 5' oligonucleotide corresponding to vector. This was performed multiple times, yielding a single 1.8-kb product that was ligated by TA cloning (Invitrogen). Non-coding ends were obtained through nested rapid amplification of cDNA ends (RACE) PCR. From overlapping cDNA clones, a complete sequence was obtained. The start was identified by a Kozak consensus sequence at the initiating methionine with two in-frame stop codons and no ATG codons upstream²⁹, and by homology to the human homologue in GenBank⁶.

Generation of antisera

Polyclonal rabbit antisera were generated against C-terminal peptides of human and wheatgerm HP68 (see Supplementary Information Fig. 3) and 19 N-terminal residues of human RNase L. HuHP68 antisera was affinity purified against HuHP68 C-terminal peptide and coupled to protein A, generating anti-HuHP68b.

Transfections, immunoprecipitation and immunofluorescence

Cells in 6-cm dishes were transfected using Gibco lipofectamine (Cos-1) or lipofectamine plus (293T) with pCMVRev and PSVGagRRE-R (1 µg each) for HIV-1 Gag expression¹⁷, with pBRUΔenv (2 µg, Fig. 3; 4 µg, Figs 1 and 5) for expression of the nearly complete HIV-1 genome¹⁶, or plasmids derived from these encoding indicated mutations. WGHP68-Tr1 was constructed by ligating cDNA encoding WGHP68 amino acids 1–378 into *NheI/XbaI* of pCDNA 3.1 (Invitrogen). Medium was collected 28 or 42 h after transfection for immunofluorescence and immunoblotting, respectively. For immunofluorescence, cells were fixed in paraformaldehyde, permeabilized with 1% triton, and incubated with mouse HIV-1 Gag antibody (1:50) and affinity-purified HuHP68 antiserum (1:2,000), followed by Cy3- and Cy2-coupled secondary antibody (Jackson) (1:200). We quantified 178 cells. In Fig. 3, rat immunoglobulin-γ was added to medium as a tracer (10 µg ml⁻¹) at collection; immunoblots were performed with Gag antibody (Dako) at 1:500, WGHP68 antiserum at 1:500, or other antisera. Bands were quantified using an immunoblot standard curve generated with known sample dilutions. For immunoprecipitations (Figs 1 and 5), cells from 6-cm dishes were collected in 300 µl NP40 buffer⁵ (containing no magnesium and 10 mM EDTA, Fig. 5), and 100 µl was immunoprecipitated with 50 µl anti-HuHP68b or beads coupled to non-immune serum. In Fig. 1a, indicated lysates were treated with RNase A (0.1 µg ml⁻¹) at 22 °C for 15 min before immunoprecipitation. In Fig. 1d, ACH-2 cells³⁰ were stimulated with phorbol myristate acetate (10 nM) for 24 h before collection. Unstimulated ACH-2 cells, producing much lower levels of infectious virus, gave the same results (data not shown). In Fig. 5b,

anti-HuHP68b was pre-incubated with the HuHP68 peptide used to generate antisera and was then dissolved in dimethylsulphoxide (200 µM), or in dimethylsulphoxide alone.

Immunodepletion-reconstitution

Wheatgerm extract (150 µl) was immunodepleted for 45 min at 4 °C with 100 µl beads coupled to antibody to WGHP68. Cell-free reactions (15 µl) were programmed using non-depleted wheatgerm or depleted wheatgerm. To some reactions containing depleted wheatgerm, WGHP68–GST, HuHP68–GST or GST alone was added (2 µl of approximately 20 ng µl⁻¹) at the start of the reaction. After 3 h at 26 °C, 1% NP40 was added and reactions underwent velocity sedimentation (5 ml, 15–60% sucrose gradients, Beckman ML550 rotor, 45 min, 129,000g). Thirty fractions, collected using a fractionator, were analysed by SDS–polyacrylamide gel electrophoresis (PAGE) and autoradiography, followed by densitometry of Gag in each lane. Graphs show average of three independent experiments (± s.e.m.). For the protease digestions, aliquots of 500S and 750S peaks were incubated for 10 min at 22 °C with or without 0.1 µg ml⁻¹ proteinase K, and analysed by SDS–PAGE and autoradiography (quantification as above).

WGHP68 and HuHP68 were subcloned into pGEX (Pharmacia) encoding N-terminal GST fusion proteins. Expression was induced with 1 mM isopropyl β-D-thiogalactopyranoside; sarcosyl (0.5%) and phenylmethylsulphonyl fluoride (PMSF) (0.75 mM) were added after sonication. Supernatant (17,000 µg) was incubated with glutathione beads and eluted with 40 mM glutathione in 50 mM Tris, pH 8.0.

Electron microscopy

Two cell-free reactions were programmed with HIV-1 Gag transcript and immunodepleted wheatgerm, and WGHP68–GST was added to one of the reactions. Cell-free reactions and medium from Cos-1 cells were transfected to produce immature HIV-1 virus¹⁷, treated with 1% NP40 to remove envelopes, and centrifuged on 2 ml 20–66% sucrose gradients (Beckman TLS55 rotor, 35 min, 135,000g). Fractions containing 750S peaks⁵ were placed on Formvar-coated grids previously incubated with Gag antibody for 10 min, fixed in half-strength Karnovsky's fixative, stained with uranyl acetate, and examined by transmission electron microscopy (Japan Electric Optics Laboratories 1010).

Received 24 May; accepted 24 September 2001.

- Boulanger, P. & Jones, I. Use of heterologous expression systems to study retroviral morphogenesis. *Curr. Top. Microbiol. Immunol.* **214**, 237–260 (1996).
- Jacobs, E., Gheysen, D., Thines, D., Francotte, M. & de Wilde, M. The HIV-1 Gag precursor Pr55gag synthesized in yeast is myristoylated and targeted to the plasma membrane. *Gene* **79**, 71–81 (1989).
- Mariani, R. *et al.* A yeast to human immunodeficiency virus type 1 assembly in murine cells. *J. Virol.* **74**, 3859–3870 (2000).
- Mariani, R. *et al.* Mouse-human heterokaryons support efficient human immunodeficiency virus type 1 assembly. *J. Virol.* **75**, 3141–3151 (2001).
- Lingappa, J. R., Hill, R. L., Wong, M. L. & Hegde, R. S. A multistep, ATP-dependent pathway for assembly of human immunodeficiency virus capsids in a cell-free system. *J. Cell Biol.* **136**, 567–581 (1997).
- Bisbal, C., Martinand, C., Silhol, M., Lebleu, B. & Salehzada, T. Cloning and characterization of a RNase L inhibitor. A new component of the interferon-regulated 2-5A pathway. *J. Biol. Chem.* **270**, 13308–13317 (1995).
- Singh, A. R., Hill, R. L. & Lingappa, J. R. Effect of mutations in Gag on assembly of immature human immunodeficiency virus type 1 capsids in a cell-free system. *Virology* **279**, 257–270 (2001).
- Hynes, G. *et al.* Analysis of chaperonin-containing TCP-1 subunits in the human keratinocyte two-dimensional protein database: further characterisation of antibodies to individual subunits. *Electrophoresis* **17**, 1720–1727 (1996).
- Willison, K. *et al.* The T complex polypeptide 1 (TCP-1) is associated with the cytoplasmic aspect of Golgi membranes. *Cell* **57**, 621–632 (1989).
- Lingappa, J. R. *et al.* A eukaryotic cytosolic chaperonin is associated with a high molecular weight intermediate in the assembly of hepatitis B virus capsid, a multimeric particle. *J. Cell Biol.* **125**, 99–111 (1994).
- Traut, T. W. The functions and consensus motifs of nine types of peptide segments that form different types of nucleotide-binding sites. *Eur. J. Biochem.* **222**, 9–19 (1994).
- Salehzada, T., Silhol, M., Lebleu, B. & Bisbal, C. Polyclonal antibodies against RNase L. Subcellular localization of this enzyme in mouse cells. *J. Biol. Chem.* **266**, 5808–5813 (1991).
- Zhou, A., Hassel, B. A. & Silverman, R. H. Expression cloning of 2-5A-dependent RNAase: a uniquely regulated mediator of interferon action. *Cell* **72**, 753–765 (1993).
- Player, M. R. & Torrence, P. F. The 2-5A system: modulation of viral and cellular processes through acceleration of RNA degradation. *Pharmacol. Ther.* **78**, 55–113 (1998).
- Martinand, C. *et al.* RNase L inhibitor is induced during human immunodeficiency virus type 1 infection and down regulates the 2-5A/RNase L pathway in human T cells. *J. Virol.* **73**, 290–296 (1999).
- Kimpton, J. & Emerman, M. Detection of replication-competent and pseudotyped human immunodeficiency virus with a sensitive cell line on the basis of activation of an integrated β-galactosidase gene. *J. Virol.* **66**, 2232–2239 (1992).
- Smith, A. J., Srinivasakumar, N., Hammarskjöld, M. L. & Rekosh, D. Requirements for incorporation of Pr160gag-pol from human immunodeficiency virus type 1 into virus-like particles. *J. Virol.* **67**, 2266–2275 (1993).
- Gheysen, D. *et al.* Assembly and release of HIV-1 precursor Pr55gag virus-like particles from recombinant baculovirus-infected insect cells. *Cell* **59**, 103–112 (1989).
- Hockley, D. J., Nermut, M. V., Grief, C., Jowett, J. B. & Jones, I. M. Comparative morphology of Gag protein structures produced by mutants of the gag gene of human immunodeficiency virus type 1. *J. Gen. Virol.* **75**, 2985–2997 (1994).
- Jowett, J. B., Hockley, D. J., Nermut, M. V. & Jones, I. M. Distinct signals in human immunodeficiency virus type 1 Pr55 necessary for RNA binding and particle formation. *J. Gen. Virol.* **73**, 3079–3086 (1992).
- Royer, M. *et al.* Functional domains of HIV-1 gag-polyprotein expressed in baculovirus-infected cells. *Virology* **184**, 417–422 (1991).
- Bukovsky, A. A., Dorfman, T., Weimann, A. & Gottlinger, H. G. Nef association with human immunodeficiency virus type 1 virions and cleavage by the viral protease. *J. Virol.* **71**, 1013–1018 (1997).

23. Pandori, M. W. *et al.* Producer-cell modification of human immunodeficiency virus type 1: Nef is a virion protein. *J. Virol.* **70**, 4283–4290 (1996).
24. Welker, R., Harris, M., Cardel, B. & Krausslich, H. G. Virion incorporation of human immunodeficiency virus type 1 Nef is mediated by a bipartite membrane-targeting signal: analysis of its role in enhancement of viral infectivity. *J. Virol.* **72**, 8833–8840 (1998).
25. Cohen, E. A., Subbramanian, R. A. & Gottlinger, H. G. Role of auxiliary proteins in retroviral morphogenesis. *Curr. Top. Microbiol. Immunol.* **214**, 219–235 (1996).
26. Madani, N. & Kabat, D. An endogenous inhibitor of human immunodeficiency virus in human lymphocytes is overcome by the viral Vif protein. *J. Virol.* **72**, 10251–10255 (1998).
27. Simon, J. H. & Malim, M. H. The human immunodeficiency virus type 1 Vif protein modulates the postpenetration stability of viral nucleoprotein complexes. *J. Virol.* **70**, 5297–5305 (1996).
28. Simon, J. H. *et al.* The regulation of primate immunodeficiency virus infectivity by Vif is cell species restricted: a role for Vif in determining virus host range and cross-species transmission. *EMBO J.* **17**, 1259–1267 (1998).
29. Kozak, M. Interpreting cDNA sequences: some insights from studies on translation. *Mamm. Genome* **7**, 563–574 (1996).
30. Folks, T. M. *et al.* Tumor necrosis factor α induces expression of human immunodeficiency virus in a chronically infected T-cell clone. *Proc. Natl Acad. Sci. USA* **86**, 2365–2368 (1989).

Supplementary Information accompanies the paper on Nature's website (<http://www.nature.com>).

Acknowledgements

Vif monoclonal antibody (TG001; Transgene) and Nef monoclonal antibody (EH1; gift of J. Hoxie) were provided by the AIDS Research and Reference Reagent Program, Division of AIDS, NIAID, National Institutes of Health. We thank J. Kucinski and F. Calayag for technical assistance; M. Hayden, T. Liegler, R. Grant and the Gladstone Institute, San Francisco, for assistance with HIV-infected cells; V. Kewalramani, D. Littman, M. Goldsmith and W. Hansen for advice or, reagents; L. Caldwell and the Electron Microscopy Laboratory at the Fred Hutchinson Cancer Research Center in Seattle; and V. Lingappa, J. Lingappa, J. Dooher, J. Overbaugh, J. M. McCune, M. Linial and R. Hegde for discussions. This work was supported by grants to J.R.L. from the National Institutes of Health AIDS Division, Pediatric AIDS Foundation, and the University of California Universitywide AIDS Research Program.

Competing interests statement

The authors declare that they have no competing financial interests.

Correspondence and requests for materials should be addressed to J.R.L. (e-mail: jais@u.washington.edu). The sequence for WGHP68 has been deposited in GenBank under accession number AY059462.

IRE1 couples endoplasmic reticulum load to secretory capacity by processing the XBP-1 mRNA

Marcella Calfon, Huiqing Zeng, Fumihiko Urano, Jeffery H. Till, Stevan R. Hubbard, Heather P. Harding, Scott G. Clark & David Ron

Skirball Institute of Biomolecular Medicine, New York University School of Medicine, New York, New York 10016, USA

The unfolded protein response (UPR), caused by stress, matches the folding capacity of endoplasmic reticulum (ER) to the load of client proteins in the organelle^{1,2}. In yeast, processing of *HAC1* mRNA by activated Ire1 leads to synthesis of the transcription factor Hac1 and activation of the UPR³. The responses to activated IRE1 in metazoans are less well understood. Here we demonstrate that mutations in either *ire-1* or the transcription-factor-encoding *xbp-1* gene abolished the UPR in *Caenorhabditis elegans*. Mammalian *XBP-1* is essential for immunoglobulin secretion and development of plasma cells⁴, and high levels of *XBP-1* messenger RNA are found in specialized secretory cells⁵. Activation of the UPR causes IRE1-dependent splicing of a small intron from the *XBP-1* mRNA both in *C. elegans* and mice. The protein encoded by the processed murine *XBP-1* mRNA accumulated during the UPR, whereas the protein encoded by unprocessed mRNA did not. Purified mouse IRE1 accurately cleaved *XBP-1* mRNA *in vitro*,

indicating that *XBP-1* mRNA is a direct target of IRE1 endonucleolytic activity. Our findings suggest that physiological ER load regulates a developmental decision in higher eukaryotes.

IRE1 is a stress-activated endonuclease resident in the ER that is conserved in all known eukaryotes. In yeast, Ire1-mediated unconventional splicing of an intron from *HAC1* mRNA controls expression of the encoded transcription factor³ and is required for upregulation of most UPR target genes^{6,7}. UPR gene expression in mammals relies largely on pancreatic ER kinase (PERK) and ATF6 (refs 8–11), which are absent from yeast. Furthermore, mammalian IRE1 proteins activate Jun amino-terminal kinase by recruiting the TRAF2 protein to the ER membrane independently of their endonucleolytic activity¹². It is unclear, therefore, whether IRE1 proteins of higher eukaryotes also signal ER stress through processing of *HAC1*-like mRNA targets. To address this issue we used a genetic strategy to identify UPR regulatory genes in *C. elegans*, a simple organism whose genome is predicted to encode homologues of all three known proximal, stress-sensing components of the metazoan UPR: *IRE1*, *PERK* and *ATF6*.

Caenorhabditis elegans has two homologues of the ER chaperone

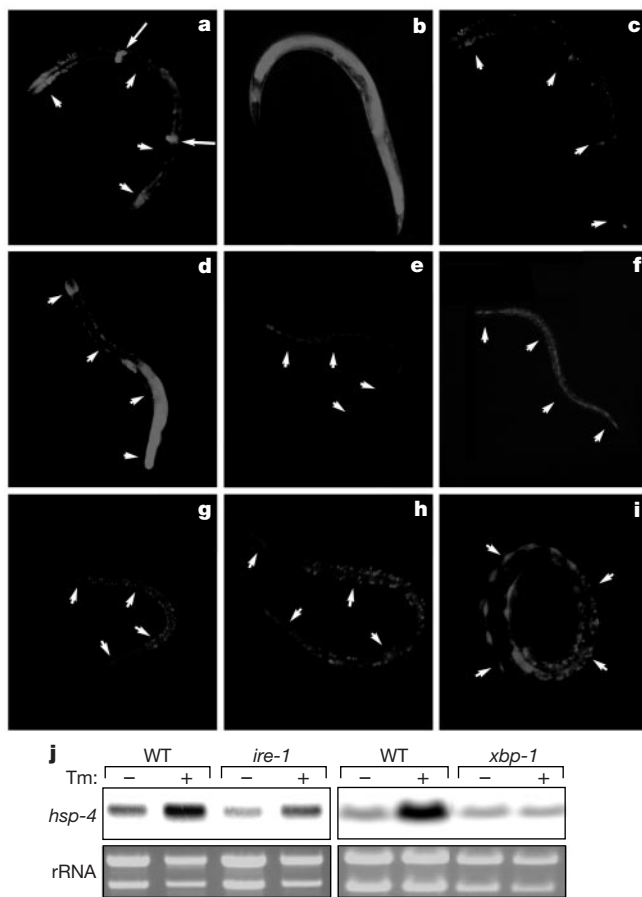


Figure 1 Identifying mutants in the *C. elegans* UPR. **a**, Fluorescent photomicrograph of an untreated adult *hsp-4::gfp(zcls4)V* transgenic animal. White arrowheads (in all panels) track the outline of the body; arrows indicate the spermatheca. **b**, An *hsp-4::gfp(zcls4)V* animal treated with tunicamycin. **c**, Tunicamycin-treated *ire-1(RNAi)III; hsp-4::gfp(zcls4)V* animal. **d**, Untreated *hsp-4::gfp(zcls4)V; upr-1(zc6)X* animal (note constitutive activation of the UPR in the posterior gut). **e**, Untreated *hsp-4::gfp(zcls4)V; upr-1(zc14)X* animal with a second mutation in *ire-1(zc14)III*. **f**, Tunicamycin-treated *ire-1(zc14)III; hsp-4::gfp(zcls4)V* animal. **g**, Untreated *hsp-4::gfp(zcls4)V; upr-1(zc6)X* animal with a second mutation in *xbp-1(zc12)III*. **h**, Tunicamycin-treated *xbp-1(zc12)III; hsp-4::gfp(zcls4)V* animal. **i**, Tunicamycin-treated *xbp-1(RNAi)III; hsp-4::gfp(zcls4)V* animal. **j**, Northern blot of *hsp-4* RNA from untreated and tunicamycin-treated (Tm) wild-type (WT), *ire-1(zc10)II* or *xbp-1(zc12)III* mutant animals. Integrity and loading of the RNA is revealed by ethidium bromide staining of the ribosomal bands. rRNA, ribosomal RNA.